

# Optimal Switched Reluctance Motor Control Strategy for Wide Voltage Range Operation

F. D'hulster , K. Stockman

Hogeschool West-Vlaanderen, dept. PIH  
Graaf Karel de Goedelaan 5, B-8500 Kortrijk (Belgium)  
phone: (+32) 56 24 12 35, fax: (+32) 56 24 12 24  
e-mail: [frederik.dhulster@howest.be](mailto:frederik.dhulster@howest.be)

I. Podoleanu , R. Belmans

KU Leuven, dept. ESAT, div. ELECTA,  
Kasteelpark Arenberg 10, B-3001 Leuven (Belgium)  
phone: (+32) 16 32 10 20fax: (+32) 16 32 19 85  
e-mail: [ronnie.belmans@esat.kuleuven.ac.be](mailto:ronnie.belmans@esat.kuleuven.ac.be)

**Abstract** — This paper describes a technique to obtain optimal torque control parameters of a switched reluctance motor (SRM). A relationship between dc-link voltage and rotor speed is used, reducing the number of control parameters. Using a nonlinear motormodel, surfaces are created describing torque, torque ripple and efficiency as function of rotor speed and the main control parameters. Next, optimization software generates optimal control parameter combinations out of these surfaces for equidistant torque-speed performance. The advantage of this technique is an offline optimization platform and the simplicity to create additional surfaces (e.g. acoustic noise, vibrations, ...).

## I. INTRODUCTION

Due to the ever increasing application demands put on switched reluctance motor drives, a flexible control strategy is gaining importance. Some applications demand a low acoustic noise or vibration level, others feature high efficiency. This paper deals with the design and implementation of an optimal control strategy for an 8/6 SRM, operating in a broad supply voltage range. Robust control must be applied for a dc-link voltage range of 115 – 325 V and a speed range of 0 – 2000 rpm.

At full motor load, a maximum torque control strategy must be used to obtain maximum mechanical power at the motor shaft. At medium load, different combinations of phase current and control angles are possible for a given reference torque. This degree of freedom enables optimization of the torque control parameters.

A complete optimization of machine geometry – converter – control of a SRM is proposed in [1] using genetic algorithms (GA) as an optimization tool. In many applications, the use of standard motor designs is preferred rather than developing a motor geometry for every new application. The motor behaviour as function of its torque control parameters is calculated only once and can serve as input for an offline optimization platform. Through a weighted sum of objective functions, the control of a standard SRM can be optimized for different applications. Figure 1 illustrates the flowchart of this procedure.

First, the basic equations for the nonlinear SRM model are explained. Next, the main parameters (N) for the torque control are derived, taking into account the relation between the dc-link voltage and the rotor speed. Then, N-dimensional surfaces are created, representing the SRM behaviour as function of the torque control

parameters. Finally, the optimal control parameters for the complete torque-speed range are determined using a genetic algorithm (GA) search tool or alternatively a “search for all” tool.

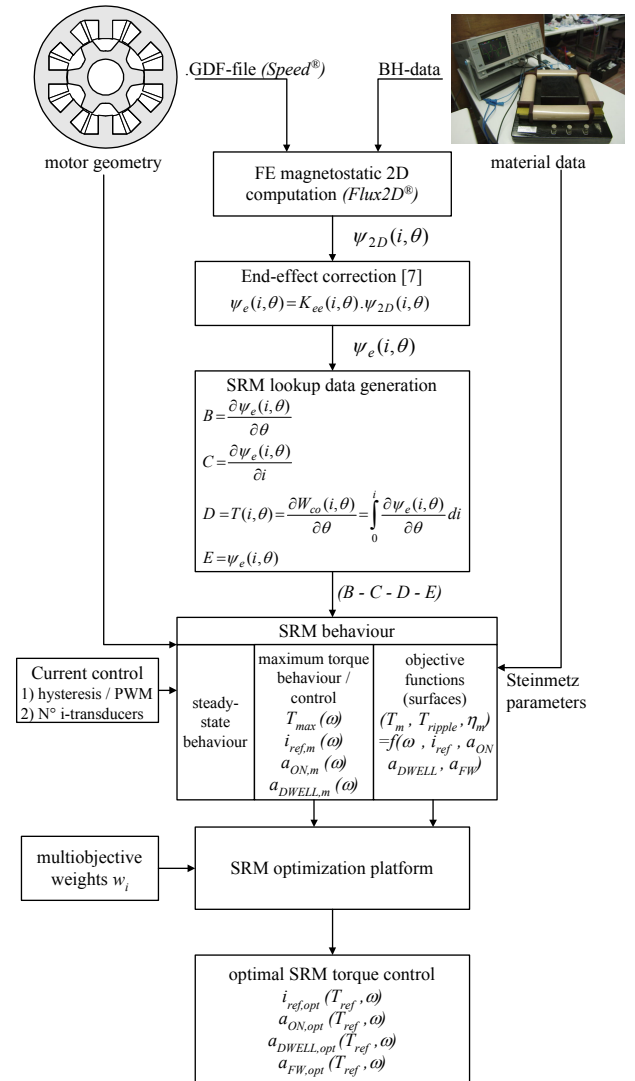


Figure 1. General flowchart of the optimal torque control of SRMs

## II. SRM SYSTEM EQUATIONS AND DRIVE MODEL

The static behaviour of a SRM can be explained by two equations, describing the current in a stator phase (1) and the instantaneous electromagnetic torque  $T$ , produced by a stator phase (2). Both equations depend on the partial derivatives of the flux-linkage  $\psi(i, \theta)$ .

$$\frac{di}{dt} = \frac{1}{\frac{\partial \psi(i, \theta)}{\partial i}} \left( u - Ri - \frac{\partial \psi(i, \theta)}{\partial \theta} \omega \right) \quad (1)$$

$$T(i, \theta) = \left. \frac{\partial W_{co}(i, \theta)}{\partial \theta} \right|_{i=cst} = \int_0^i \frac{\partial \psi(i, \theta)}{\partial \theta} \cdot di \quad (2)$$

with:

- $\frac{\partial \psi(i, \theta)}{\partial i} = p_i(i, \theta)$ : phase inductance [H]
- $\frac{\partial \psi(i, \theta)}{\partial \theta} = p_\theta(i, \theta)$ : back-emf coefficient
- $\omega$  : rotor speed [rad/s]
- $u$  : phase voltage [V]
- $i$  : phase current [A]
- $R$  : phase resistance [ $\Omega$ ]

This single-phase behaviour, represented by four matrices as function of rotor position and phase current, is deduced from a magnetostatic finite element analysis (Figure 2). The unaligned rotor position is set to 30° and the aligned to 60°. Figure 3 shows the single-phase static behaviour of the motor, further used in this paper.

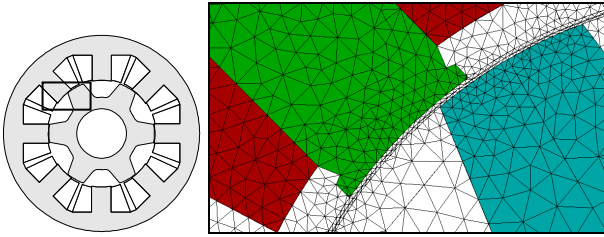


Figure 2. Geometry and 2D finite element model (Flux2D®)

SRM control optimization is only possible using an accurate dynamic motor model, including saturation, iron loss estimation and torque ripple calculation, combined with a drive model using the appropriate torque and current control (hysteresis or PWM). Both motoring and generating mode are supported, for different phase current sensing. Superposition of single-phase SRM-modelling, using lookup tables with 2D magnetostatic finite element flux-linkage data, is described in [4]. This model is extended with iron loss calculation, based on the modified Steinmetz equation [5]. The Steinmetz parameters, describing the iron losses function for sinusoidal excitation are measured on a standard Epstein frame. Further in this paper, only motoring operation is considered.

If ventilation and friction losses are neglected, efficiency and torque ripple for motoring operation are:

$$\eta_m = \frac{P_m}{P_m + P_{Cu} + P_{Fe}} \quad (3)$$

$$T_{ripple} = \frac{\max(T) - \min(T)}{T_m} \quad (4)$$

with:

- $P_m$  : mechanical power [W]
- $P_{Cu}$  : Joule losses [W]
- $P_{Fe}$  : iron losses [W]
- $T_m$  : average torque [Nm]

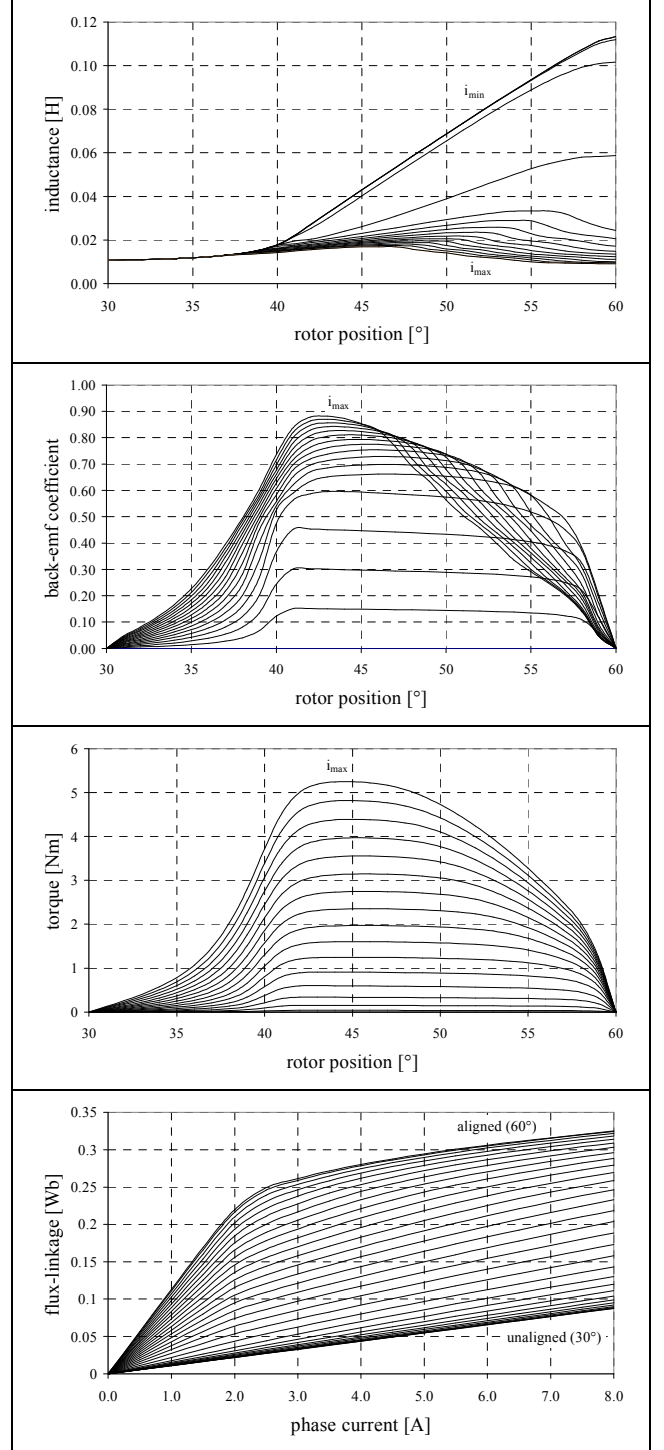


Figure 3. Single-phase SRM lookup data

### III. SRM TORQUE CONTROL

Unlike dc-machines or rotating field machines, in SRMs no direct link exists between torque and current, in this way complicating its control. This is linked to the fact that even in steady state the stored magnetic energy in the machine is not constant. A basic torque controller (Figure 4) consists of lookup tables with the control parameters (turn-on angle  $a_{ON}$ , dwell angle  $a_{DWELL} = a_{OFF} - a_{ON}$ , freewheeling angle  $a_{FW}$  and reference current  $i_{ref}$ ), determined according to an optimization criterion. The current can be controlled using a hysteresis or PWM control technique. With a PWM current controller the system produces less acoustic noise due to the fixed switching period, but its PI control parameters must be selected carefully. In addition to this basic structure, also different torque ripple reduction principles can be implemented, of which examples in [6] and [8].

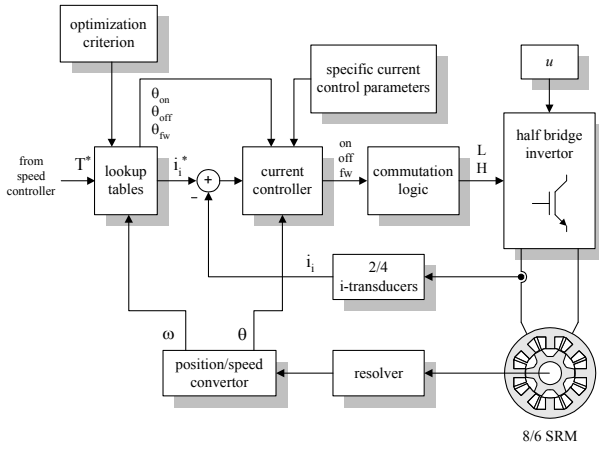


Figure 4. Basic SRM torque control structure

### IV. VOLTAGE-SPEED RELATIONSHIP

So far, not much research is done on the control of SRMs under different supply voltage conditions. Reference [3] proposes a maximum torque control strategy during short disturbances in the dc-link voltage due to voltage sags or load transients. For steady state behaviour, [2] describes the similarity between supply voltage decrease and rotor speed increase on the current waveform of SR generators. This reduces the number of parameter sets in the drive.

Equation (1) can be rewritten to:

$$\frac{di}{d\theta} = \frac{1}{\frac{\partial \psi(i, \theta)}{\partial i}} \left( \frac{u - Ri}{\omega} - \frac{\partial \psi(i, \theta)}{\partial \theta} \right) \quad (5)$$

Relation (5) states that, for a given phase current behaviour, a relation exists between the phase voltage and the rotor speed:

$$\frac{u - Ri}{\omega} = cst \quad (6)$$

For a given voltage  $u$ , speed  $\omega(u)$  and reference

torque, the optimal control parameters can be obtained from the parameter set, defined for  $u_{ref}$ , using an equivalent rotor speed  $\omega(u_{ref})$ :

$$\omega(u_{ref}) = \frac{(u_{ref} - Ri_{ref})}{(u - Ri_{ref})} \cdot \omega(u) \quad (7)$$

with: -  $i_{ref}$  : reference phase current [A]  
-  $u_{ref}$  : reference phase voltage [V]

An example of this relation between supply voltage and rotor speed is given in Figure 5 with the numerical simulation results in Table I.

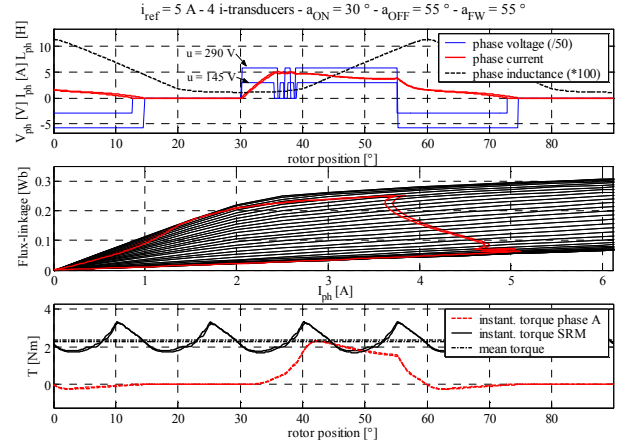


Figure 5. Comparison of current and torque behaviour for voltage-speed combinations of the same parameter set ( $\omega_1 = 432 \text{ rad/s}$ ,  $u_1 = 290 \text{ V}$ ,  $\omega_2 = 200 \text{ rad/s}$ ,  $u_2 = 145 \text{ V}$ )

TABLE I. Numerical steady state simulation results

$\omega$ [rad/s]	$u$ [V]	$T_m$ [Nm]	$P_m$ [W]	$P_{Cu}$ [W]	$P_{Fe}$ [W]	$\eta_m$
432	290	2.28	928	119	59	0.839
200	145	2.34	450	122	20	0.760

If the control is to be optimized for a supply voltage range  $[u, u_{ref}]$  in a motor speed range  $[0, \omega_{max}]$ , then the equivalent optimal control parameters must be calculated for the supply voltage  $u_{ref}$  in a speed range  $[0, \omega_{max} \cdot \frac{u_{ref} - Ri_{ref}}{u - Ri_{ref}}]$ .

### V. SRM MAXIMUM TORQUE CONTROL

When the speed or position controller demands maximum torque performance from the motor, no freedom is left for optimization. Both turn-on and dwell angle are determined to maximize the loop-surface during energy conversion [3]. In this paper only motoring operation is elaborated. The turn-on angle is calculated to reach the reference current at the start of pole-overlap:

$$a_{ON} = a_{ref} - \frac{\omega \cdot L_u \cdot i_{max}}{u_{ref} - p_{\theta}(i_{ref}, a_{ref}) \cdot \omega} \quad (8)$$

with: -  $a_{ref}$ : start of inductance increase (pole-overlap)  
-  $L_u$ : inductance at unaligned rotor position [H]

For the full rotor speed range, maximum torque control parameters are obtained, using the maximum available phase current  $i_{max}$ . Based on this maximum available torque at every rotor speed, the torque-speed plane is divided into equidistant torque-speed reference curves (Figure 6). An important feature is the equidistance between torque references. This enables to design a stable speed or position controller. Intersection between different reference torque-speed lines would inevitably result in unstable operating points. The control angles and the SRM behaviour for the maximum torque control are illustrated in Figure 7. Maximum Torque Control parameters are not obtained using the optimization algorithm because finding the parameters for the unique peak value of a surface is not an obvious task for any search tool.

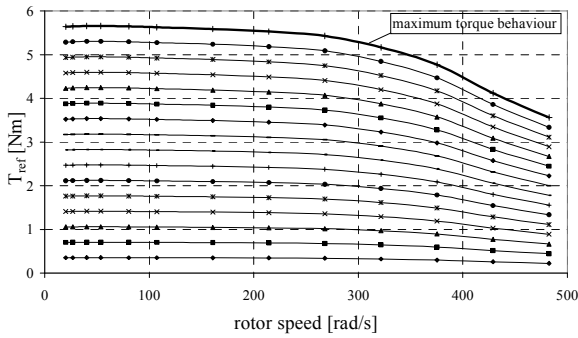


Figure 6. Equidistant reference torque curves, related to the maximum torque behaviour for  $u_{ref}$

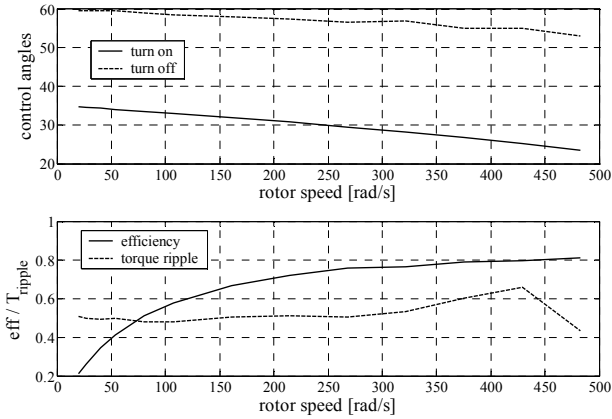


Figure 7. SRM maximum torque control angles and behaviour for  $u_{ref}$  and  $i_{max}$

## VI. SRM OBJECTIVE FUNCTIONS (SURFACES)

Objective functions, describing the SRM behaviour as a function of the control parameters, are the input functions of the optimization platform. Different functions or surfaces can be calculated, using the nonlinear motor model, e.g. efficiency, torque ripple, acoustic noise ... Besides those surfaces, allowing an optimization criterion, the torque surface is also needed

as a constraint function to satisfy the reference torque demand. Figure 8 shows the surfaces of the torque, efficiency and torque ripple for a fixed turn-on angle and rotor speed. Different combinations of the parameters can result in the same torque production, allowing optimization of the parameters for a given reference torque constraint.

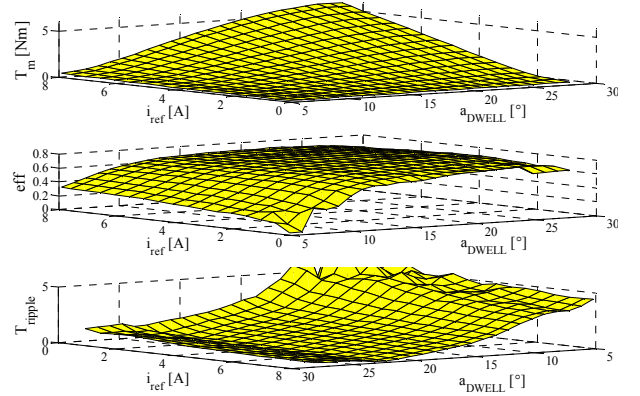


Figure 8. Torque, efficiency and torque ripple for constant turn-on angle and rotor speed ( $a_{ON} = 30^\circ$ ;  $\omega_{ref} = 160.85$  rad/s)

## VII. OPTIMAL CONTROL PARAMETERS DETERMINATION

As pointed out, for each speed and reference torque, the appropriate input variables  $i_{ref,opt}$ ,  $a_{ON,opt}$  and  $a_{DWELL,opt}$  must be determined in such a way that the overall performance matches an optimization criterion. For SRMs, the optimality condition is in general determined by straightforward requirements with regard to the efficiency, torque ripple or acoustic noise. The efficiency should be maximized, the torque ripple and acoustic noise minimized.

All objective functions are combined into a single value function, called generic cost ( $c$ ). For example, the generic cost function of efficiency and torque ripple is:

$$c = w_1 (1 - \eta_m) + w_2 \left( \frac{T_{ripple}}{\max(T_{ripple})} \right) \quad (9)$$

The optimal solution is a combination of input variables for which the cost function is minimized, for a given speed and reference torque. Although the surfaces of Figure 8 seem relatively smooth, this is not the general behaviour. In practice, noise on the surface results in many combinations of input variables with the same value for the cost function. As a direct consequence, only numerical algorithms able to find a global solution can be used, avoiding local minima. As a general constraint with regard to the final implementation, the chosen algorithm should always find the solution within a reasonable time. Moreover, the solution should be found from any initial starting point.

There are several algorithms to determine the desired minimum, but only two were implemented. The first attempt uses a genetic algorithm (GA) as it is characterized by a high probability to find a global minimum. However, for a few operating points, no useful solution is found. A second algorithm (“search for all”) takes all possible combinations of input variables with a constant step and determines the constrained minimum. This method is straightforward to implement and a solution is found for every operating point. The calculation time is function of the number of parameters and the step size. A GA search method has the disadvantage that a solution is not guaranteed and that one particular solution is searched, without taking into account that this combination could be useful for other torque reference values. The direct “search for all” method calculates the objective and constraint function values for a parameter combination and tests the cost for all torque reference values. This strongly reduces the computation time.

With a weight of 0.5 for efficiency and 0.5 for torque ripple, the optimal control parameters are presented in Figures 9 – 11, using the “search for all” algorithm.

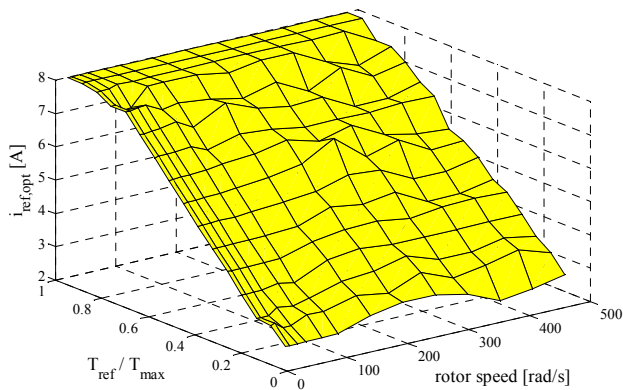


Figure 9. Optimal reference current  $i_{ref,opt}$  for  $u_{ref}$  ( $w_1 = 0.5 ; w_2 = 0.5$ )

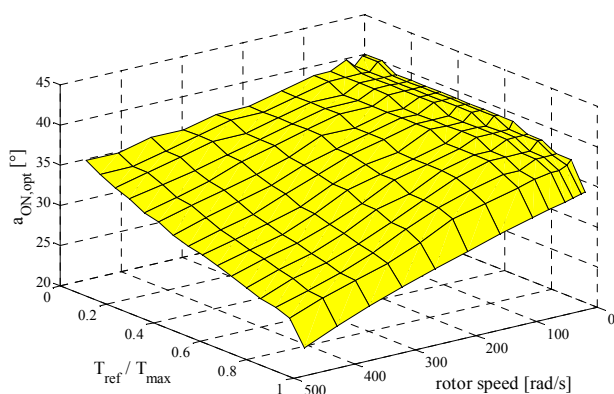


Figure 10 Optimal turn on angle  $a_{ON,opt}$  for  $u_{ref}$  ( $w_1 = 0.5 ; w_2 = 0.5$ )

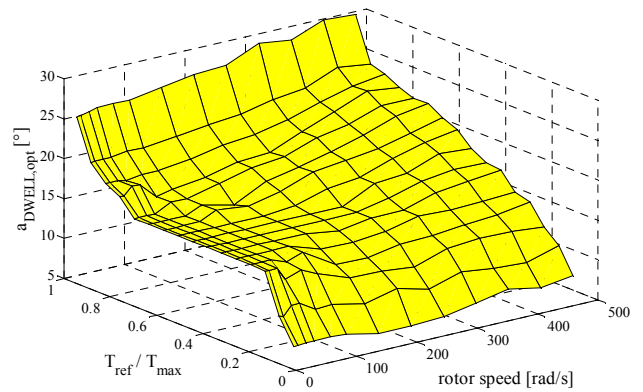


Figure 11 Optimal dwell angle  $a_{DWELL,opt}$  for  $u_{ref}$  ( $w_1 = 0.5 ; w_2 = 0.5$ )

## VIII. MEASUREMENT RESULTS

The optimal control parameters, described in chapter VII are programmed into a SRM drive and its behaviour is measured on a test setup with load machine. Validating if the control is really optimal is not easy. The model accuracy is verified by means of torque and efficiency measurements. Figure 12 represents the measured torque-speed performance, according to the reference torque values for every rotor speed. No intersection between the lines occurs, resulting in a stable position or speed controller. Efficiency is determined by measuring the electrical power, supplied to the motor, and the mechanical shaft torque. Efficiency measurements as function of reference torque and rotor speed are compared with simulations in Figure 13 and Figure 14.

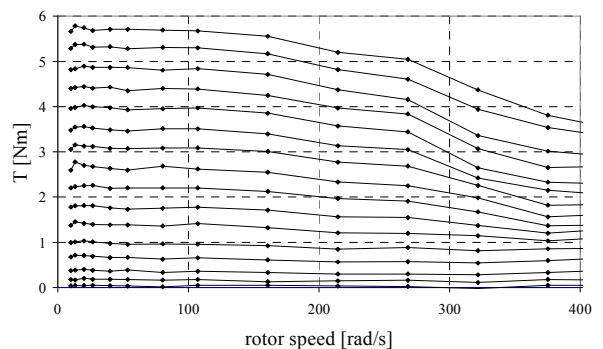


Figure 12 Measured torque -speed performance with optimal control parameters for  $u_{ref}$  ( $w_1 = 0.5 ; w_2 = 0.5$ )

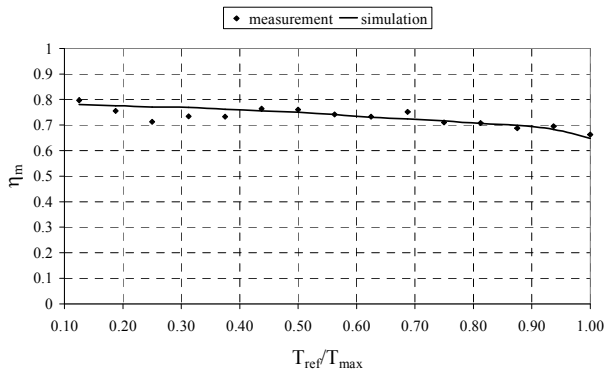


Figure 13 Measured and simulated motor efficiency as function of reference torque ( $u_{ref}$ ;  $\omega = 214$  rad/s)

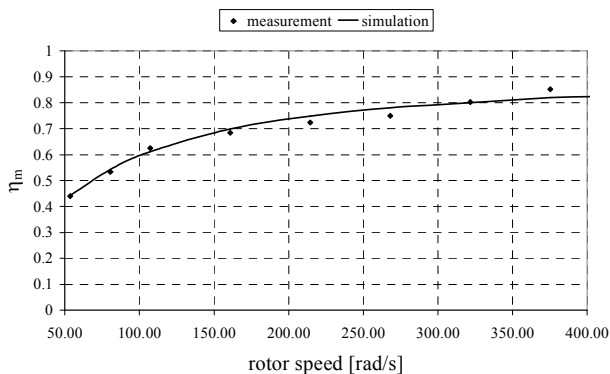


Figure 14 Measured and simulated motor efficiency as function of rotor speed ( $u_{ref}$ ;  $T_{ref} = 0.5T_{max}$ )

## IX. CONCLUSIONS

Different torque control strategies can be implemented in SRM drives, operating at varying supply voltage conditions. A technique is presented to obtain optimal SRM torque control parameters, according to a weighted optimization criterion. The dc-link voltage is not considered as a fundamental parameter due to its analogy with rotor speed. Using a nonlinear SRM drive model, the behaviour is stored in N-dimensional surfaces, serving as objective and constraint functions for the optimization platform. The objective functions in this paper are limited to motor efficiency and torque ripple but can easily be extended with acoustic noise or temperature. The surfaces are calculated only once for each motor geometry and different control parameter sets can be obtained for different application demands.

## Acknowledgement

The authors wish to thank the Flemish Government (IWT) for granting the research project "Bepaling van de optimale stuur- en regelparameters voor systemen met SR-motor aandrijving. Ontwerp van een ontwikkelingsplatform." (IWT 020343). The general optimisation work is part of the IUAP/PAI P4/20 project "Coupled problems" sponsored by the Belgian Federal Government.

## REFERENCES

- [1] Lomonova E., Matveev A., "Application of genetic algorithm for design of switched reluctance drives", *European Conference on Power Electronics and Applications (EPE 2003)*, 2-4 September 2003, Toulouse, France.
- [2] Inderka R. B., Menne M., De Doncker R. W., "Generator operation of a switched reluctance machine drive for electric vehicles", *EPE journal*, vol. 11, N° 3, August 2001.
- [3] D'hulster F., Stockman K., Belmans R., "Maximum torque control strategy for switched reluctance motors during dc-link disturbances", *European Conference on Power Electronics and Applications (EPE 2003)*, 2-4 September 2003, Toulouse, France.
- [4] D'hulster F., Stockman K., Desmet J., Belmans R., "Advanced nonlinear modelling techniques for switched reluctance machines", *IASTED International Conference on Modelling, Simulation and Optimization (MSO 2003)*, 2-4 July 2003, Banff, Alberta, Canada, pp. 44-51
- [5] Reinert J., Inderka R. B., De Doncker R. W., "A novel method or the prediction of losses in switched reluctance machines", *European Conference on Power Electronics and Applications (EPE 97)*, Trondheim, 1997, pp. 3608-3612.
- [6] Husain I., Ehsani M., "Torque ripple minimization in switched reluctance motor drives by PWM current control", *IEEE transactions on power electronics*, vol. 11, N° 1, 1996, pp. 83-88.
- [7] Matveev A., Kuzmichev V., Lomonova E., "A new comprehensive approach to estimation of end-effects in switched reluctance motors", *International Conference on Electrical Machines (ICEM 2002)*, 26-30 August 2002, Brugge, Belgium.
- [8] Inderka R. B., De Doncker R. W., "DITC - Direct instantaneous torque control of switched reluctance drives", *IEEE Industry applications conference, 37th IAS Annual meeting*, Pittsburgh, Pennsylvania, USA, October 13-18, 2002, pp. 1605-1609.
- [9] Miller T. J. E., "Electronic control of switched reluctance machines", *Newnes Power Engineering Series*, Oxford, 2001, pp. 92-97.